

Total Cross Sections of $e^+e^- \rightarrow$ hadrons and pQCD Tests^a

K. Kang^{b,c,d}, V. V. Ezhela^e, S. K. Kang^d,
S. B. Lugovsky^e, M. R. Whalley^f, O. V. Zenin^e
(COMPETE (e^+e^-) Collaboration)

^b*Physics Department, Brown University, Providence, R.I. 02912, U.S.A.*

^c*Institute of Physics & Applied Physics, Yonsei University, Seoul 120-749, Korea*

^d*School of Physics, Korea Institute for Advanced Study, Seoul 130-012, Korea*

^e*COMPAS Group, IHEP, Protvino, Russia*

^f*HEPDATA Group, Durham University, Durham, UK*

In the light of recent muon ($g - 2$) result by the E821 experiment at BNL, the importance of and interest in the total hadronic cross sections in e^+e^- collisions and $R(e^+e^- \rightarrow \text{hadrons})$ have been heightened. We report on the integrated data compilation of available data of $e^+e^- \rightarrow \text{hadrons}$, transformed to a unique and meaningful style that implements the pure QED radiative corrections, from the PPDS and HEPDATA databases by the COMPETE Group. In particular, the continuum data sets are extracted where the direct comparison of the parton models and different variants of the pQCD corrections can be made and which will be useful for the future refinements of $\alpha_s(Q^2)$ and $\alpha_{QED}(Q^2)$.

1 Introduction

In spite of the tremendous experimental and phenomenological efforts that have been devoted to the study of the hadronic production in e^+e^- collisions, it is simply the state of arts that there is no truly integrated view on the experimental situation for the main observable such as the total cross section for the reaction $e^+e^- \rightarrow \text{hadrons}$ and the ratio

$$R = \frac{\sigma(e^+e^- \rightarrow \text{hadrons})}{\sigma(e^+e^- \rightarrow \mu^+\mu^-)_{QED}}$$

To be specific, we note that some experiments published only the data of the cross sections, σ , while others did only the R data. The situation is more complicated as for the QED radiative effects to the data, because various data sets have been corrected by different ways and to different degrees. For example, in constructing R , two different forms of theoretical calculations had been used, i.e., one with $\alpha_{QED}(0)$ and another taking into account the accepted form of evolution of $\alpha_{QED}(Q^2)$ then. Furthermore, some data were never published in numerical form and have been read by compilers from graphs.

^aPresented by one of us (K.K.) at the 6th Workshop on Non-perturbative QCD, American University of Paris, 5-9 June 2001. Report No. BROWN-HET-1097

Determination of the precision data for $\sigma(e^+e^- \rightarrow \text{hadrons})$ and R has been a continuing endeavor in particle physics as new precision experiments became feasible and has received renewed interests recently. Some of the recent experimental activities that revived the interest in the data of $\sigma(e^+e^- \rightarrow \text{hadrons})$ and R are: the precision electroweak data that allowed us to calculate the radiative corrections and extract the QED coupling constant; the anomalous magnetic moment of the muon ($g - 2$) which showed some 2.6σ deviation from the standard model prediction initially compared to the new result of the E281 experiment at BNL¹; and the τ decay data. In the analysis of all these experiments, the hadronic contribution is the major source of the ambiguity and errors. A new controversy of the the light-by-light scattering contribution (as for the sign)² to the vacuum polarization, the dominant leading contribution to the hadronic contribution reinforces only the need of precise values of these data.

The aim of this work³ is to prepare a comprehensive compilation of σ and R transformed, whenever possible, to a unique, and meaningful, style by implementing the pure QED radiative corrections. The second aim is to construct a procedure to extract “continuum data sets” where the direct comparison of the parton model with different variants of the pQCD corrections can be made. In selecting data for the compilation we use the expert assessments from various recent reviews and works dealing with precise estimation of running $\alpha_{QED}(Q^2)$ and $\alpha_s(Q^2)$ (see, e.g., Ref.⁴, Ref.⁵, and Ref.⁶).

2 Data Selection and Normalizations

All published data were extracted in numerical form from the PPDS RD⁷ database and from the Reaction Database of HEPDATA system⁸. Certain data were excluded based on the following exclusion criteria:

- All preliminary data were excluded;
- Data obtained under incomplete kinematical conditions, and not extrapolated to the complete kinematic region, were excluded;
- Data in the form of dense energy scans are omitted if the authors published in addition the data averaged over wider energy bins.

The data sets that survived the above exclusion criteria were subdivided into the following six categories:

σ_1^{sd} : Cross section data corrected in the original works for the contributions of two-photon exchange diagrams, the initial state bremsstrahlung and

for the initial state vertex loops, but not corrected for the vacuum polarization contribution to the running α_{QED} . These “**semi-dressed**” cross sections take into the full γ/Z propagator with vacuum polarization effects.

σ_2^{sd} : Cross section data radiatively corrected according to the procedure of Bonneau and Martin⁹ in the original works. This procedure included radiative corrections for the initial state radiation, electronic vertex correction, and the correction for the electronic loop in the photon propagator. Thus it partially took into account the vacuum polarization effects. To obtain from these cross sections the “**semi-dressed**” ones we rescale σ_2^{sd} by a factor $1/(1 - \Delta\alpha_{QED}^e(s))^2$.

R_3^{bare} : Data on R obtained from measurements of the “**semi-dressed**” (σ_2^{sd}) cross-section divided by the point-like muonic cross section with fixed $\alpha_{QED} = \alpha_{QED}(0)$ in the works. To obtain the “**bare**” R -parameter we rescale these data by the factor $(\alpha_{QED}(0)/\alpha_{QED}(s))^2/(1 - \Delta\alpha_{QED}^e(s))^2$.

R_4^{bare} : Data on R obtained from measurements of the “**semi-dressed**” (σ_1^{sd}) cross section divided by the point-like muonic cross section, in the original works, but with the running $\alpha_{QED}(s)$ which thus obtained the “**bare**” R -ratio.

σ_5^{sd} : LEP I cross section data at the Z peak not corrected for initial state radiation and electronic QED vertex loops, and LEP II – III cross section data at $\sqrt{s} > 130$ GeV with a cut $s'/s = 1 - (\sqrt{s}/2)(1 - 0.7225)$, $\sqrt{s'}$ being an effective mass of the propagator. These data were rescaled to the “**semi-dressed**” cross section σ_1^{sd} as follows. First, the theoretical cross sections^b σ_{cut}^{th} and σ_{Born}^{th} were calculated using ZFITTER 6.30 package¹⁰, assuming the values of the standard model parameters from PDG¹¹. Here σ_{cut}^{th} means the cross section measured with cuts applied in the particular experiment and determined from the fit by ZFITTER and σ_{Born}^{th} denotes the theoretical cross section, calculated by ZFITTER in the Improved Born Approximation (IBA), that includes the full γ/Z propagator with vacuum polarization effects. Then the experimental cross section was multiplied by the factor $\sigma_{Born}^{th}/\sigma_{cut}^{th}$.

σ_6^{sd} : Low energy data ($2m_\pi < E_{cm} < 2$ GeV), the treatment of which requires special consideration.

All the cross sections $\sigma(e^+e^- \rightarrow hadrons)$ in this range are obtained by summing the exclusive channels and therefore give only a lower estimate of the total hadronic cross section. Below 1 GeV we summed up the 2π and 3π

^bValues for σ_{cut}^{th} were calculated using ZFITTER subroutine ZUTHSM with argument settings according to the cuts applied in the LEP I-II-III measurements. Values for σ_{born}^{th} were calculated by the same subroutine but with the special flag switching it to calculate the IBA cross sections.

channels using a linear interpolation of the individual data sets within specific energy regions and combined them to give the total hadron cross sections in these regions. The errors were calculated according to these interpolation and summation procedures.

Such an approach works well if all the data are evenly distributed over \sqrt{s} and have comparable errors. Otherwise it may cause false resonance-like structures in the total cross section in the given \sqrt{s} interval if there are few points of the leading channel with large errors, and if this interval is filled more densely by the points of the minor channels. Such false structures are possible and likely to occur for the exclusive channel data in the range $1.4 < \sqrt{s} < 2$ GeV, where we summed the contributions from the channels $\geq 3hadrons$, $\pi^+\pi^-$, K^+K^- , and $K_S K_L$. To avoid such false structure we have determined the sum of exclusive channels not for all points, where at least one channel is measured, but in a fewer number of points, for which the channels yielding the major contributions are identified. In other aspects the summation procedure was the same as the one used for the data below 1 GeV. The exclusive sum data in the $0.81 < \sqrt{s} < 1.4$ GeV region are taken from the paper¹⁸. The data used for the exclusive channel summation around ϕ resonance ($0.997 < \sqrt{s} < 1.028$ GeV) were corrected for the initial state radiation, electronic vertex loops and leptonic 1-loop insertions into the γ propagator in these data. We have properly rescaled these data. In the remaining 0.81–1.4 GeV data they applied QED-corrections using the Bonneau and Martin⁹ prescription and all these data points were rescaled as in the σ_2^{sd} -case.

3 Data Compilations on σ^{sd} and R^{bare}

After selecting and rescaling the data, normalized to the full γ/Z contributions, we assemble the complete data set of the total hadronic cross sections σ^{sd} , in accordance with the symbolic relation

$$\sigma^{sd} = \sigma_1^{sd} \cup \sigma_2^{sd} \cup \sigma_5^{sd} \cup \sigma_6^{sd} \cup \left[(R_3^{bare} \cup R_4^{bare}) \cdot \sigma_{QED}^{\mu\mu} \text{ pole, running } \alpha_{QED} \right]$$

and the complete data set for the R -ratios

$$R^{bare} = \frac{\sigma(e^+e^- \rightarrow hadrons)}{\sigma(e^+e^- \rightarrow \mu^+\mu^-)_{QED \text{ pole, running } \alpha_{QED}}}.$$

As described above, in creating compilations which are uniform in the sense of implementing a standardized pure QED radiative corrections to the

“raw” published experimental data, the values of the running $\alpha_{QED}(s)$ and $\Delta\alpha_{QED}^e(s)$ are needed. The numerical values of these parameters and estimates for their uncertainties are described in the next section. Both compilations are stored and maintained in the PPDS CS database, corresponding to the record of the original data but with the rescaled data points. Also stored are brief descriptions of the applied conversion procedures in the special comment in each record. The σ and \mathbf{R}^{bare} compilations obtained by this procedure are shown in the Figs. 1 and 2, respectively.

4 α_{QED} , $\Delta\alpha_{QED}^{had}$ and the Continuum Region

4.1 Theoretical Relations.

The QED running coupling constant $\alpha_{QED}(s)$ can be expressed in the form

$$\alpha_{QED}(s) = \frac{\alpha(0)}{1 - \Delta\alpha(s)},$$

$$\Delta\alpha(s) = \Delta\alpha^{had}(s) + \Delta\alpha^{lep}(s), \quad (1)$$

where $\Delta\alpha^{had}(s)$, $\Delta\alpha^{lep}(s)$ are hadronic and leptonic contributions to the QED vacuum polarization, respectively.

$\Delta\alpha^{lep}(s)$ is well approximated in perturbative QED by the sum of leptonic loop contributions,

$$\Delta\alpha^{lep}(s) = \sum_{l=e,\mu,\tau} \frac{\alpha(0)}{3\pi} \left[\ln \frac{s}{m_l^2} - \frac{5}{3} + \mathcal{O}\left(\frac{m_l^2}{s}\right) \right]. \quad (2)$$

The situation with respect to $\Delta\alpha^{had}(s)$ is more complicated due to an essentially non-perturbative nature of the strong interaction at low energies. Using the unitarity and the analyticity of the scattering amplitudes, one can express $\Delta\alpha^{had}(s)$ in the form of a subtracted dispersion relation

$$\Delta\alpha^{had}(s) = -\frac{\alpha(0)s}{3\pi} \int_{4m_\pi^2}^{\infty} \frac{R(s')ds'}{s'(s' - s - i0)}, \quad (3)$$

where $R(s)$ is the “bare” hadronic R -ratio.

This relation allows to effectively evaluate the $pQCD$ R -ratios in the continuum \sqrt{s} intervals in terms of experimental R data containing the non-perturbative effects.

We have evaluated the dispersion integral in two parts,

$$\Delta\alpha^{had}(s) = -\frac{\alpha(0)s}{3\pi} \left[\int_{4m_\pi^2}^{s_{cut}} ds' \frac{R_{bare}^{data}(s')}{s'(s'-s-i0)} + \int_{s_{cut}}^{\infty} ds' \frac{3\sum_q Q_q^2(1 + \frac{\alpha s(s')}{\pi})}{s'(s'-s-i0)} \right], \quad (4)$$

where the first integral was calculated numerically as a trapezoidal sum over the weighted average of experimental R points in the range $2m_\pi < \sqrt{s'} < \sqrt{s_{cut}} = 19.5 \text{ GeV}^c$

Our numerical evaluation procedure is in general similar to the one applied in Ref. ^{4, d}

We obtained $\Delta\alpha^{had}(M_Z^2) = 0.0274 \pm 0.0004(\text{exp.})$, which is consistent with the results 0.027382 ± 0.000197 and 0.027612 ± 0.000220 , obtained with two methodically different low energy data sets in Ref. ¹⁵. This result is preliminary and serves only as a guarantee against egregious errors in our procedure. The procedure of $\Delta\alpha^{had}(M_Z^2)$ evaluation requires further refinement.

In the parton model, before QCD corrections are applied, the R -ratio is given by

$$R = 3 \sum_q R_q^0 = 3 \sum_q \left[\beta_q \left(1 + \frac{1}{2}(1 - \beta_q^2)\right) \cdot R_q^{VV} + \beta_q^3 R_q^{AA} \right], \quad (5)$$

where

$$\begin{aligned} R_q^{VV} &= e_e^2 e_q^2 + 2e_e e_q \bar{v}_e \bar{v}_q \text{Re}\chi + (\bar{v}_e^2 + \bar{a}_e^2) \bar{v}_q^2 |\chi|^2 \\ R_q^{AA} &= (\bar{v}_e^2 + \bar{a}_e^2) \bar{a}_q^2 |\chi|^2 \end{aligned} \quad (6)$$

with

$$\chi = \frac{1}{16\bar{s}^2 \bar{c}^2} \frac{s}{(s - M_Z^2 + iM_Z \Gamma_Z)}$$

^cChoosing s_{cut} we must satisfy at least the following two requirements:

- 1) s_{cut} should lie well above all the hadronic resonances, i.e. 1-loop perturbative QED can be used to calculate hadronic vacuum polarization at $s > s_{cut}$;
- 2) there should be enough densely distributed experimental points at $s < s_{cut}$ for the trapezoidal numerical evaluation of the dispersion integral over $2m_\pi < \sqrt{s} < \sqrt{s_{cut}}$. As there are few experimental points in the interval $13 < \sqrt{s} < 30 \text{ GeV}$, $\sqrt{s_{cut}} = 19.5 \text{ GeV}$ appears to be a compromise between these requirements.

^dAs the calculation of R_{bare}^{data} from the original σ and R data (see Section 1) in turn requires the evaluation of $\Delta\alpha^{had}(s)$, we applied the following simple iterative procedure: Taking as the zeroth approximation $R(s)$ as obtained from the original data using 1-loop perturbative $\alpha_{QED}(s)$, we evaluate $\Delta\alpha^{had(1)}(s)$, which in turn is used to compute the next approximation of $R(s)$ from the original data, and then evaluate the integral again to obtain $\Delta\alpha^{had(2)}(s)$, and so on. This process converges well and after the two iterations the algorithmic error of $\Delta\alpha^{had}(s)$ in the continuum region is much less than the error coming from the experimental data uncertainty.

$$\begin{aligned}
\bar{v} &= \sqrt{\rho} (T_3 - 2Q\bar{s}^2) \\
\bar{a} &= \sqrt{\rho} T_3 \\
\rho &= 1 + \frac{3\sqrt{2}G_F}{16\pi^2} m_t^2 + \dots \quad .
\end{aligned} \tag{7}$$

Here \bar{s}^2, \bar{c}^2 are effective $\sin^2 \theta_W, \cos^2 \theta_W$ defined through renormalized couplings at $s = M_Z^2$ and

$$M_Z^2 = \frac{\pi \cdot \alpha_{QED}(M_Z^2)}{\sqrt{2}G_F \cdot \rho \cdot \bar{s}^2 \cdot \bar{c}^2} . \tag{8}$$

The dominant correction to ρ originates from t -quark loops in W and Z propagator due to the large mass splitting between the b and t quarks which represents an $SU(2)$ breaking in the unified electroweak theory.

Including QCD loops, R is given by (see, e.g., Ref.¹⁶ and Ref.¹⁷):

$$\begin{aligned}
R &= 3 \sum R_q \\
&= 3 \sum \left[R_q^0 + \left(\frac{\alpha_s}{\pi} + \left(\frac{\alpha_s}{\pi} \right)^2 (1.9857 - 0.1153N_f) \right. \right. \\
&\quad \left. \left. - \left(\frac{\alpha_s}{\pi} \right)^3 (6.6368 + 1.2001N_f + 0.0052N_f^2 + 1.2395(\sum Q_q)^2) \right) \right. \\
&\quad \left. \times (f_1 R_q^{VV} + f_2 R_q^{AA}) \right]
\end{aligned} \tag{9}$$

where N_f is the number of active quark flavors. The coefficients f_1 and f_2 depend only on the quark velocity $\beta = (1 - 4M_q^2/s)^{1/2}$, where M_q is the threshold for the flavor production of quark q . Schwinger¹³ calculated f_1 in the QED context, which is accurate enough for our purposes:

$$f_1 = \beta_q \left(1 + \frac{1}{2}(1 - \beta_q^2) \right) \frac{4\pi}{3} \left(\frac{\pi}{2\beta_q} - \frac{3 + \beta_q}{4} \left(\frac{\pi}{2} - \frac{3}{4\pi} \right) \right) \tag{10}$$

The coefficient f_2 (which have no counterpart in QED) were calculated by Jersak et al¹², which we parameterized as

$$f_2 = a_4 \beta_q^4 + a_3 \beta_q^3 + (1 - a_4 - a_3) \beta_q^2 \tag{11}$$

with $a_4 = -16, a_3 = 17$. From equations (5), (6), (9) one can easily see that the relative error of R is less than 10^{-7} at $\sqrt{s} = 10$ GeV and less than 0.5% at the Z pole, even if we allow a 100% error for f_2 . As we did not use Z pole data in our fits, this could not be a source of large theoretical errors.

In the massless quark limit, $f_1 = f_2 = 1$. However, at $\sqrt{s} = 35$ GeV for b quark one has $\beta = 0.963$ and thus $f_1 \simeq 1.3$ and $f_2 \simeq 1.7$. Indeed, such a

parameterization of mass effects is valid in QCD only in $\mathcal{O}(\alpha_s)$ order. Now the correct parameterization is known up to $\mathcal{O}(\alpha_s^3)$ order (see, e.g., Ref.¹⁶ and Ref.¹⁷), but it has not been implemented yet into our programme. It may be that it results in large enough discrepancies just in the region where α_s/π becomes large.

We used the following three-loop parameterization for α_s (see, e.g., Ref.¹⁴):

$$\ln(Q^2/\Lambda_{\overline{MS}}^2) = \frac{4\pi}{\beta_0\alpha_s} - \frac{1}{2} \frac{\beta_1}{\beta_0^2} \ln \left[\left(\frac{4\pi}{\beta_0\alpha_s} \right)^2 + \frac{\beta_1}{\beta_0^2} \left(\frac{4\pi}{\beta_0\alpha_s} \right) + \frac{\beta_2}{\beta_0^3} \right] - \frac{1}{\Delta} \left(\frac{\beta_1}{\beta_0^2} \right) \tan^{-1} \left[\frac{1}{\Delta} \left(\frac{\beta_1}{\beta_0^2} + \frac{2\beta_2}{\beta_0^3} \left(\frac{\beta_0\alpha_s}{4\pi} \right) \right) \right] \quad (12)$$

with

$$\begin{aligned} \beta_0 &= 11 - 2N_f/3, \\ \beta_1 &= 2(51 - 19N_f/3), \\ \beta_2 &= (2857 - 5033N_f/9 + 325N_f^2/27)/2, \\ \Delta &= \sqrt{4\beta_2/\beta_0^3 - \beta_1^2/\beta_0^4}. \end{aligned} \quad (13)$$

The onset of a new flavor q takes place at $Q^2 = \mu_q^2 \equiv 4m_q^2$, where, in general, $m_q \neq M_q$. There are five different $\Lambda_{\overline{MS}}(N_f)$ corresponding to $N_f = 2, 3, 4, 5, 6$ above the appropriate quark thresholds. To sew up α_s at the thresholds we need to use a matching condition for Λ 's: $\alpha_s(Q^2)$ is determined by fixing, say, $\alpha_s(M_Z^2)$, which is the parameter determined from the fits in our work.

We solved this equation at given Q^2 numerically by rewriting it in the form $x = f(x)$, where $x = 4\pi/(\beta_0\alpha_s)$. It enabled us to obtain correct α_s even at $Q^2/\Lambda^2 \sim 1$, where the expansion by powers of leading logarithms is no more valid (see, e.g., Ref.⁵). At $Q^2/\Lambda^2 \gg 1$ both methods yield the same result (see Fig. 4).

4.2 Preliminary Fit Results

In order to check the consistency of the description of the data on

$$R = \sigma(e^+e^- \rightarrow \text{hadrons})/\sigma(e^+e^- \rightarrow \mu^+\mu^-)$$

with the theoretical R -ratio expression we have performed several fits using a sub-set of the compiled data set of R which is applicable to the perturbative domain. This sub-set of the data is defined by the the following steps:

1. The low energy region $2m_\pi < \sqrt{s} < 2$ GeV is completely excluded;
2. All the data above 70 GeV are excluded, as we did not attempt to perform any fits of Z pole parameters M_Z , Γ_Z , \bar{s}_W^2 and M_{top} . This exclusion is justified because the data above 70 GeV weakly depend on $\alpha_s(M_Z)$ and the quark masses and thus their influence on the fit of Z pole parameters would be rather negligible;
3. Data covering the narrow hadronic 1^{--} resonances, $J/\psi(1S)$, $\psi(2S)$, $\psi(3770)$, $\Upsilon(1S)$, $\Upsilon(2S)$, $\Upsilon(3S)$, $\Upsilon(4S)$, $\Upsilon(10860)$ and $\Upsilon(11020)$ are completely excluded. (The visible widths of these resonances are determined by the machine energy spread $\Delta E_{beam} \sim 10$ MeV.);
4. Also completely excluded are the SLAC-SPEAR-MARK-1 data in the $2.6 \text{ GeV} < \sqrt{s} < 7.8 \text{ GeV}$ range. These data systematically lie $\simeq 15\%$ above other experiments in the same interval.

We distinguished the $\gamma^* \rightarrow q\bar{q}$ production threshold quark masses M_q from the QCD quark “masses” m_q determining the energy scale of the onset of the new flavour q in the running of $\alpha_s(s)$. After performing the exclusions 1) – 4) we fixed $\alpha_s(M_Z)$, M_Z , Γ_Z , \bar{s}_W^2 , M_q ($q = u, d, s, t$), m_q ($q = u, d, s, c, b, t$) at the values shown in the Table 1, leaving just M_c and M_b as free parameters. Another essential feature of our fit **(I)** was that we retained as free parameters the left and right boundaries of the interval $[\sqrt{s_1}, \sqrt{s_2}]$, $3.0 \leq \sqrt{s_1} \leq 3.670$ GeV, $3.870 \leq \sqrt{s_2} \leq 5.0$ GeV, which was to be excluded from the data set in the process of χ^2/dof minimization itself.^e. Thus, the number of the degrees of freedom was also variable during this fit, for which the standard MINUIT¹⁹ program is used. Such a χ^2/dof minimization procedure cancelled possible arbitrariness in the exclusions of broad resonances in the region above $c\bar{c}$ threshold.

In the fit **(II)** we released $\alpha_s(M_Z)$ free, fixing at the same time the excluded region $\sqrt{s} = 3.09 \div 4.44$ GeV. M_c , M_b were fixed at their fitted values obtained in the fit **(I)**. Fit **(II)** gives somewhat high value $\alpha_s(M_Z) = 0.128 \pm 0.032$.

^eNarrow ψ family resonances between 3 and 4 GeV were excluded by default. Somewhat controversial is the question, whether the gaps between ψ 's can be really treated as the continuum regions. R ratio demonstrates no step up until $\sqrt{s} = 3.9 - 4.0$ GeV, just at the left knee of the broad $\psi(4040)$ resonance, where the continuum approximation of R does not work. Nevertheless, this step results in the fitted c -quark mass $M_c = 1.971$ (see fit **(III)** in the Table 1)

5 Summary. Assessed Data Compilations.

In summary:

- We have created two complementary computerized “raw” data compilations on σ and R with data presented as in the original publications in all cases except the low energy subsample. In the low energy region, where there are no direct measurements of the total cross section, we obtain estimates of the total cross section either as the sum of exclusive channels or as the sum of the two-body exclusive channels with the data on $e^+ e^- \rightarrow \geq 3 \text{ hadrons}$.
- On the basis of above two data sets we have created compilations of data on σ^{sd} and R^{bare} with one-to-one correspondence between the data points. Where necessary the data have been rescaled to the standard style of implementing the pure QED radiative corrections to the initial state and to the photon propagator to produce a data set which is suitable to test the parton model with pQCD corrections to R^{bare} , and to be able to obtain more reliable estimates for $\Delta\alpha_{QED}^{had}(Q^2)$.
- From the total data compilation on R^{bare} we have defined a “continuum” data compilation sub-set which can be used in conjunction with other data in the refinements of the $\alpha_s(Q^2)$ evolution and possibly in the global fits of the Standard Model.

All data files are accessible by:

<http://wwwppds.ihep.su:8001/comphp.html>

and will be accessible from the PDG site soon.

Acknowledgments

This work is supported in part by the U.S. DoE Contract DE-FG02-91ER4068-Task A, the grant RFBR-01-07-90392 and a grant from PPAR(UK). One of us (KK) would like to thank Bruce McKellar for discussions and also KIAS and Yonsei University, Seoul, Korea for the hospitality during the sabbatical year 2000 - 01.

Table 1. Fit results in the defined “continuum” regions. Adjustable parameters are shown in bold.

Parameter	I	II	III
$\alpha_s(M_Z^2)$	0.1181	0.128(32)	0.126(37)
M_Z	91.187	91.187	91.187
Γ_Z	2.4944	2.4944	2.4944
\overline{s}^2	0.23117	0.23117	0.23117
M_t	174.3	174.3	174.3
M_u	0.140	0.140	0.140
M_d	0.140	0.140	0.140
M_s	0.492	0.492	0.492
M_c	1.500(18)	1.5	1.9710(1)
M_b	5.23 ± 1.16	5.23	6.0 ± 1.4
m_u	0.003	0.003	0.003
m_d	0.006	0.006	0.006
m_s	0.120	0.120	0.120
m_c	1.2	1.2	1.2
m_b	4.2	4.2	4.2
m_t	174.3	174.3	174.3
Excluded	$2m_\pi \div 2.0$ 3.093 ÷ 3.113	$2m_\pi \div 2.0$	$2m_\pi \div 2.0$ 3.093 ÷ 3.113 3.684 ÷ 3.688 3.670 ÷ 3.870
	3.175(247) ÷ 4.319(105)	3.09 ÷ 4.44	4.000 ÷ 4.400
\sqrt{S}	9.450 ÷ 9.470	9.450 ÷ 9.470	9.450 ÷ 9.470
intervals	10.000 ÷ 10.025	10.000 ÷ 10.025	10.000 ÷ 10.025
	10.34 ÷ 10.37	10.34 ÷ 10.37	10.34 ÷ 10.37
	10.52 ÷ 10.64	10.52 ÷ 10.64	10.52 ÷ 10.64
	10.75 ÷ 10.97	10.75 ÷ 10.97	10.75 ÷ 10.97
	11.00 ÷ 11.20	11.00 ÷ 11.20	11.00 ÷ 11.20
	70 ÷ 188.7	70 ÷ 188.7	70 ÷ 188.7
χ^2/dof	0.690	0.665	0.822

References

1. H. N. Brown *et al.*, Phys. Rev. Lett. **86** (2001) 2227.
2. M. Knecht and A. Nyffeler, hep-ph/0111058; M. Knecht *et al.*, hep-ph/0111059.
3. O. V. Zenin, V. V. Ezhela, K. Kang, S. K. Kang, S. B. Lugovsky and M.R. Whalley, hep-ph/0110176, Brown-HET-1262 and IHEP 2001-25, in which further details and complete references can be found.
4. S. Eidelman and F. Jegerlehner, Z. Phys. C **67** (1995) 585 [hep-ph/9502298].
5. I. Hinchliffe and A. V. Manohar, Ann. Rev. Nucl. Part. Sci. **50** (2000) 643 [hep-ph/0004186].
6. Z.G. Zhao, Int. J. Mod. Phys. A **15** (2000) 3739.
7. <http://wwwppds.ihep.su:8001/ppds.html>
8. <http://durpdg.dur.ac.uk/hepdata/>
9. G. Bonneau and F. Martin, Nucl. Phys. B **27** (1971) 381.
10. D. Bardin, P. Christova, M. Jack, L. Kalinovskaya, A. Olchevski, S. Riemann and T. Riemann, Comput. Phys. Commun. **133** (2001) 229 [hep-ph/9908433]. ZFITTER 6.30 Fortran code is available at http://www.ifh.de/~riemann/Zfitter/zfitr6_30.uu .
11. D. E. Groom *et al.*, [Particle Data Group Collaboration], Eur. Phys. J. C **15** (2000) 1.
12. J. Jersak, E. Laermann and P. M. Zerwas, Phys. Lett. B **98** (1981) 363.
13. J. Schwinger, "Particles, Sources And Fields." Addison-Wesley, 1970. 3v.
14. R. Marshall, Z. Phys. C **43** (1989) 595.
15. A. D. Martin, J. Outhwaite and M. G. Ryskin, Phys. Lett. B **492** (2000) 69 [hep-ph/0008078].
16. K. G. Chetyrkin, J. H. Kuhn and A. Kwiatkowski, Phys. Rept. **277** (1996) 189.
17. K. G. Chetyrkin, R. V. Harlander and J. H. Kuhn, Nucl. Phys. B **586** (2000) 56 [hep-ph/0005139].
18. S. I. Dolinsky *et al.*, [VEPP-2M, ND Collaboration], Phys. Rept. **202** (1991) 99.
19. F. James and M. Roos, Comput. Phys. Commun. **10** (1975) 343.

Figures

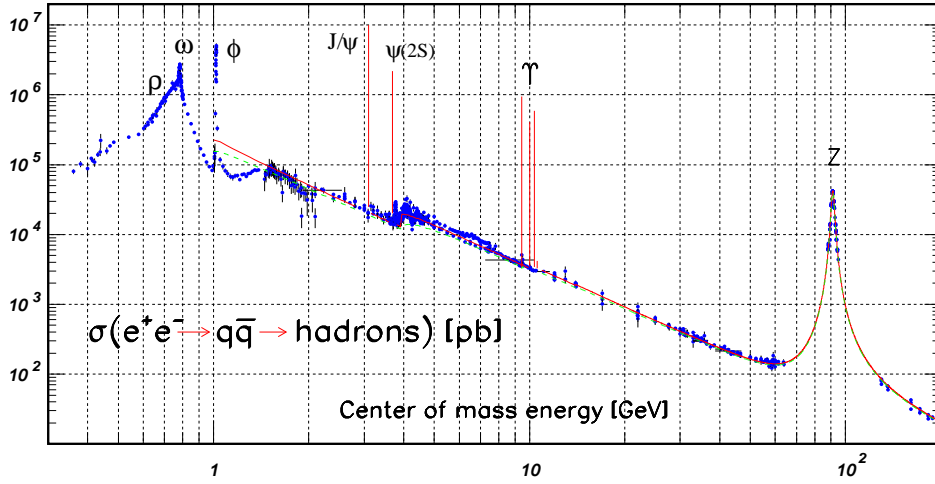


Figure 1: World data on the total cross section of $e^+e^- \rightarrow \text{hadrons}$. The experimental data on J/ψ , $\psi(2S)$, and $\Upsilon(nS), n = 1, 4$ resonances is not shown. Curves are an educational guide. Solid curve is the prediction of the cross section in the three-loop QCD approximation with non-zero quark masses. Dashed curve is a “naive” quark parton model prediction.

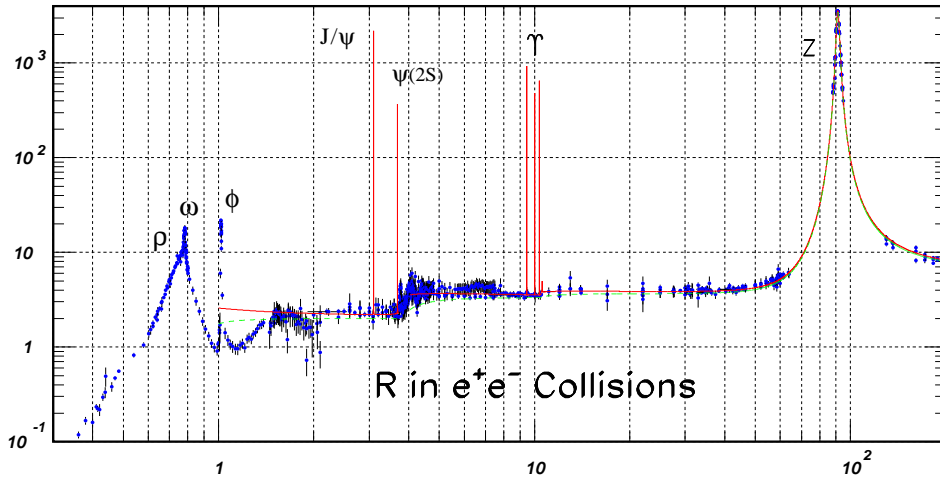


Figure 2: R -ratio. Data set is the same as in Figure 1. Solid curve is the R -ratio prediction in the three-loop QCD approximation with non-zero quark masses. Dashed curve is a “naive” quark parton model prediction for the ratio parameter R .

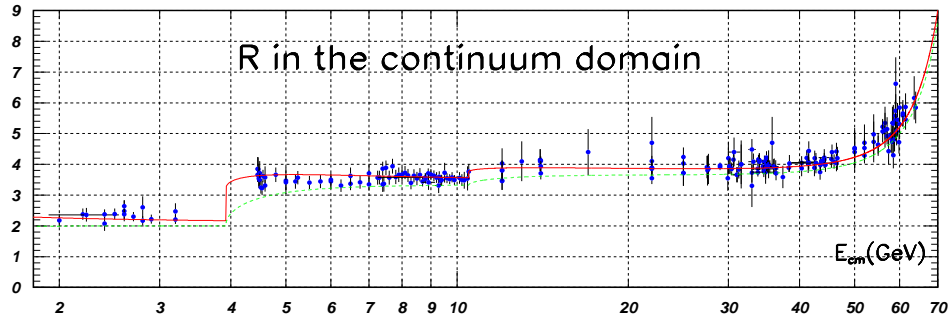


Figure 3: Data set used for the preliminary fits. Curves are the same as in Figure 2.

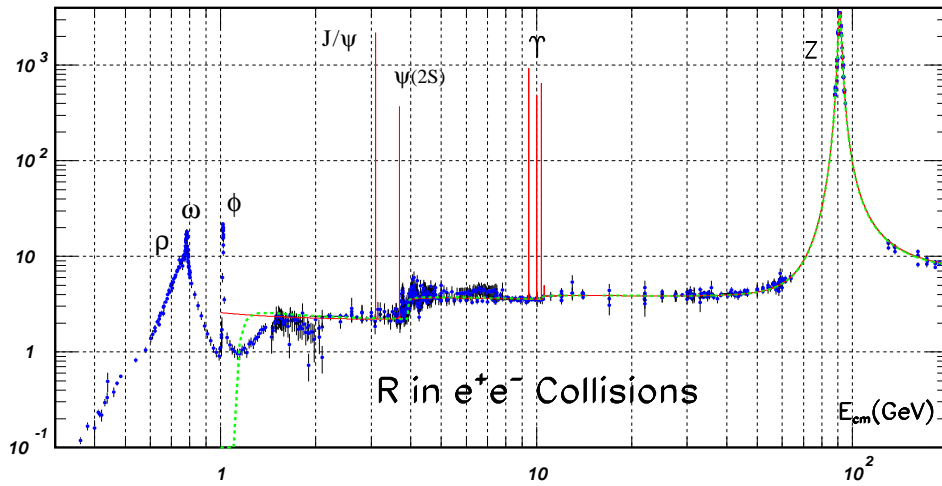


Figure 4: Comparison of R parameters obtained with $\alpha_s(s)$, evaluated by our numerical method (solid curve) and by the method described in [5] (dashed curve).